

SemHARQ: Semantic-Aware HARQ for Multi-task Semantic Communications

Jiangjing Hu, Fengyu Wang*, Wenjun Xu, *Senior Member, IEEE*, Hui Gao, *Senior Member, IEEE*, and Ping Zhang, *Fellow, IEEE*

Abstract—Intelligent task-oriented semantic communications (SemComs) have witnessed great progress with the development of deep learning (DL). In this paper, we propose a semantic-aware hybrid automatic repeat request (SemHARQ) framework for the robust and efficient transmissions of semantic features. First, to improve the robustness and effectiveness of semantic coding, a multi-task semantic encoder is proposed. Meanwhile, a feature importance ranking (FIR) method is investigated to ensure the important features delivery under limited channel resources. Then, to accurately detect the possible transmission errors, a novel feature distortion evaluation (FDE) network is designed to identify the distortion level of each feature, based on which an efficient HARQ method is proposed. Specifically, the corrupted features are retransmitted, where the remaining channel resources are used for incremental transmissions. The system performance is evaluated under different channel conditions in multi-task scenarios in Internet of Vehicles. Extensive experiments show that the proposed framework outperforms state-of-the-art works by more than 20% in rank-1 accuracy for vehicle re-identification, and 10% in vehicle color classification accuracy in the low signal-to-noise ratio regime.

Index Terms—Semantic communications, semantic-aware HARQ, feature distortion evaluation, feature importance ranking.

I. INTRODUCTION

IN the era of Internet of Everything (IoE), communications among humans, machines, objects, and intelligent agents enable intelligent services to individuals and industries. As a result, the requirements for communication systems to effectively convey the intended information are increased. Conventional communication systems focus on the successful transmissions of bits but ignore the meanings of messages, facing critical challenges to support the aforementioned applications over limited communication resources [1–3]. To solve this issue, semantic communications (SemComs), which transmit the intention-related semantics, can significantly reduce

the amount of transmission data while ensuring the system performance. Consequently, the efficiency of communication is improved effectively. Meanwhile, with the development of artificial intelligence (AI), deep learning (DL) has shown its superiority in semantic representation, compression and recovery, which has been widely used in task-oriented SemComs [4, 5].

To guarantee the reliability of semantic transmissions, most of the current DL-based SemCom systems transmit task-related semantics and identify semantic errors by joint source-channel coding (JSCC) [6, 7]. Particularly, Bourtsoulatze *et al.* propose a JSCC technique for image transmission, which directly maps the image pixel values to the complex-valued channel input symbols [6]. Furthermore, besides transmitting semantics in an end-to-end (E2E) manner, a multi-user cooperative semantic framework based on JSCC is proposed to exploit the correlations among users in [7]. However, the above SemCom systems are designed with a fixed coding rate, incapable of transmitting semantics adaptively according to the dynamic channel conditions. To overcome this problem, a variable length coding method is proposed based on dynamic neural networks in [8]. Meanwhile, a policy network is trained additionally in [9] to select a portion of the encoded feature vector based on the signal-to-noise ratio (SNR). Nevertheless, the robustness of semantic recovery is limited in the above systems due to the lack of precise process of semantic errors.

To improve the error correction ability in communication systems, hybrid automatic repeat request (HARQ) is commonly used in conventional communications [10, 11]. Specifically, a cyclic redundancy check (CRC) error detection technique is combined with retransmissions to improve transmission reliability at the data link layer. Nevertheless, the meanings of information are ignored in the above method, making it unable to handle semantic errors. Therefore, to further enhance the robustness and efficiency of SemComs, semantic retransmission schemes have been studied [12–16]. In [12], the data sample is thoroughly retransmitted in a DL-based communication network when the received semantic information is not sufficient to complete the task. A channel output feedback is further incorporated into the retransmission mechanism in [13] to improve the reconstruction quality. Although constantly retransmitting messages can improve the performance of specific intelligent task, the efficiency in resource utilization is too low for practical usage. Therefore, incremental transmission methods are further incorporated to improve the transmission efficiency. Specifically, multiple incremental transmissions are supported by different autoen-

This work was supported in part by the National Natural Science Foundation of China under Grant 62301069 and 62293485, and in part by the China Scholarship Council (*Corresponding author: Fengyu Wang*).

Jiangjing Hu is with the State Key Laboratory of Networking and Switching Technology, Beijing University of Posts and Telecommunications, Beijing 100876, China (e-mail: hujiangjing@bupt.edu.cn).

Fengyu Wang is with the School of Artificial Intelligence, Beijing University of Posts and Telecommunications, Beijing 100876, China (e-mail: fengyu.wang@bupt.edu.cn).

Wenjun Xu and Ping Zhang are with the State Key Laboratory of Network and Switching Technology, Beijing University of Posts and Telecommunications, Beijing 100876, China, and also with the Peng Cheng Laboratory, Shenzhen 518066, China (e-mail: wjxu@bupt.edu.cn, pzhang@bupt.edu.cn).

Hui Gao is with the Key Laboratory of Trustworthy Distributed Computing and Service, Ministry of Education, Beijing University of Posts and Telecommunications, Beijing 100876, China (e-mail: huigao@bupt.edu.cn).

coders in [17] to reduce semantic transmission error. To further simplify the network architecture, a unified single decoder is proposed in [9] to exploit the incremental knowledge (IK) obtained from retransmission. Besides the text and image transmission, an incremental redundancy HARQ framework is investigated for video conferencing with a semantic error detector [18]. However, the above works retransmit the same messages simply or directly transmit incremental redundancy triggered by task performance, having no insight into the specific distortion from the channel fading and noise. Consequently, the error detection on the semantic feature dimension is always ignored, where the features that are successfully received and decoded are probable to be transmitted again, decreasing the efficiency of resource utilization. At the same time, the receiver may fail to recover critical semantics that are previously transmitted when only incremental transmissions are involved without considering retransmissions, degrading the system performance.

Moreover, to ensure the transmission of critical semantics with a higher priority, the impact of different importance levels of semantic features has been investigated [19–22]. Wang *et al.* evaluate the importance of each semantic triple using an attention network [20, 21]. Meanwhile, the importance diversity among semantic features is estimated in [22] from an information theory perspective, where an entropy model is set on the latent space. Nevertheless, the above measurements cannot be associated with the semantic task performance directly, degrading the task efficiency.

Overall, to realize robust and scalable semantic transmissions, in this paper, we propose a semantic-aware HARQ (SemHARQ) framework for multi-task semantic communications. The major contributions of this work are summarized as follows:

- First, to avoid unnecessary retransmissions, a feature distortion evaluation (FDE) network is proposed to differentiate the distortion extents of the received features. The corrupted features are then identified and retransmitted, and meanwhile, the remaining resources are utilized to transmit the incremental semantics for better performance.
- Then, to further improve the transmission efficiency, a feature importance ranking (FIR) method is designed for multi-task SemComs. Specifically, a multi-task semantic encoder is proposed [23–26], where the correlated semantics among different tasks are extracted jointly, making the semantic coding more robust and efficient than existing single-task coding [27–30]. Moreover, the semantic importance levels are further evaluated by measuring the sensitivity of task performance to different features, where the gradients of the task performance w.r.t. the features are considered [31].
- Finally, to enhance the scalability of the proposed SemHARQ, the amount of semantics at each transmission is adaptively adjusted. Specifically, the length of the semantic feature vector to be transmitted is determined by the channel conditions. During retransmission, besides the features that failed to be reconstructed in previous transmissions, the incremental features are also transmit-

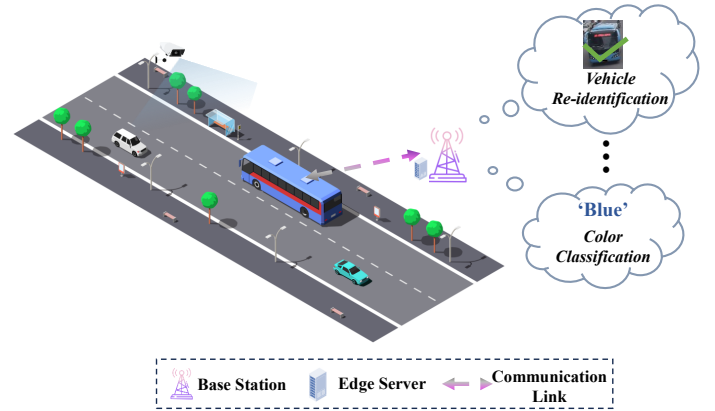


Fig. 1: The scenario of the multi-task intelligent transportation systems.

ted in descending order of importance to fully utilize channel resources.

- Extensive simulations are conducted to validate the effectiveness of the proposed SemHARQ. Numerical results demonstrate that SemHARQ outperforms the traditional HARQ and state-of-the-art semantic-aware HARQ methods, especially at the low SNR regime. To the best of our knowledge, this is the first HARQ method that realizes semantic feature-level retransmission considering semantic importance evaluation.

The remainder of this paper is organized as follows. Section II introduces the system model of the proposed SemHARQ. The architecture and principle of the FDE network and FIR method are illustrated in Section III. In Section IV, the process and training strategy of the SemHARQ are presented. Numerical results of the proposed system are demonstrated in Section V. Finally, Section VI concludes this paper.

II. SYSTEM MODEL

In this section, the system model of SemHARQ is introduced. Specifically, K intelligent tasks are executed simultaneously in intelligent transportation scenarios, and the inputs of the system are assumed to be vehicle images, as shown in Fig. 1. Note that the system can be readily extended to other scenarios and modalities. First, the semantic features are extracted and then transmitted to the receiver after scalable selection according to the importance levels. Then, the SemHARQ is triggered after receiving the semantic features from the channel. After all the transmissions, the concatenated feature vector is decoded by a joint source-channel decoder (JSC-Decoder) and multiple semantic decoders. Finally, the multiple tasks are performed by different task performers.

A. Transmitter

As shown in Fig. 2, the input images denoted as $\mathbf{x} \in \mathbb{R}^{\tilde{B} \times W \times H}$ are encoded by a multi-task semantic encoder, where \tilde{B} is the batch size, and W, H are the width and height of an image, respectively. The semantic features are extracted as $\mathbf{s} \in \mathbb{R}^N$, where N is the number of features in \mathbf{s} . Then, a JSC-Encoder encodes \mathbf{s} as $\mathbf{f} \in \mathbb{C}^L$, where L is the length

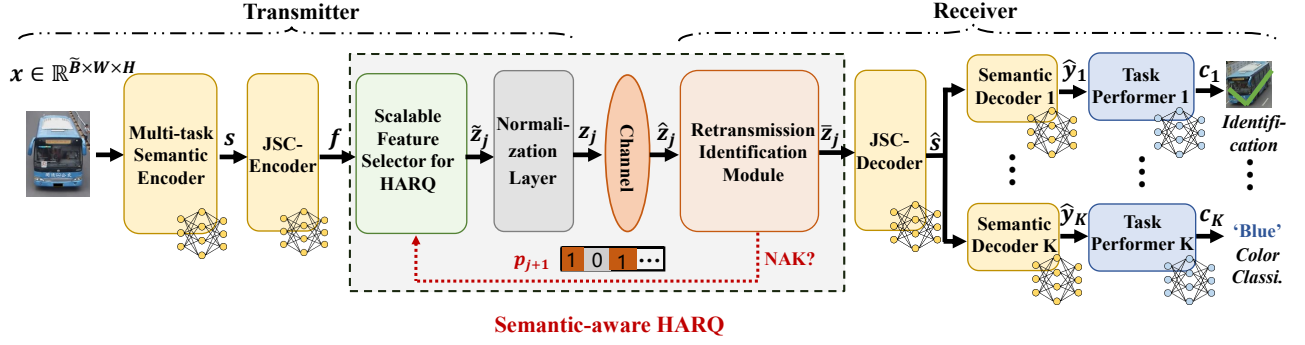


Fig. 2: The framework of the proposed SemHARQ.

of the feature vector. Afterwards, the feature vector selected by a scalable feature selector for HARQ is represented as $\tilde{z}_j \in \mathbb{C}^B$, where B is the number of features to be transmitted according to channel state information (CSI), j is the number of retransmissions. The value of B is determined by the transmission bandwidth in a single time slot so that the length of the transmitted feature vector can be scalably adjusted according to the channel conditions. Finally, the average power control is utilized to normalize the input signals of the channel at each transmission, which is shown as

$$z_j = \sqrt{PB} \frac{\tilde{z}_j}{\|\tilde{z}_j\|_2}, \quad (1)$$

where P is the average power.

Furthermore, z_j is sent and passes through a stochastic physical channel. The channel output can be represented as

$$\hat{z}_j = \mathbf{h}z_j + \mathbf{n}, \quad (2)$$

where $\mathbf{n} \in \mathbb{C}^B$ denotes the white Gaussian noise, the value of which follows $n_i \sim \mathcal{CN}(0, \sigma^2)$. $\mathbf{h} \in \mathbb{C}^B$ represents the fading coefficient of the channel. In this paper, the Rician channel is considered. The fading coefficient follows $\mathcal{CN}\left(\sqrt{r}/(r+1), 1/(r+1)\right)$, where r is set to 2.

B. Receiver

At the receiver, \hat{z}_j is measured by a retransmission identification module to detect if the retransmission is required. If \hat{z}_j passes the detection, it will be directly concatenated with the previously received features and the concatenated vector is denoted as $\bar{z}_j = [\hat{z}_1, \dots, \hat{z}_j]$. Otherwise, the received \hat{z}_j will be evaluated by the FDE network to generate a binary feedback vector p_{j+1} , indicating which features in \hat{z}_j are needed to be retransmitted. Such retransmissions will be repeated until the success of multi-task or the maximum times of retransmission is reached. After all the transmissions, the concatenated vector is decoded as $\hat{s} \in \mathbb{R}^N$ by the JSC-Decoder. \hat{s} is then recovered to $[\hat{y}_1, \hat{y}_2, \dots, \hat{y}_K]$ by multiple semantic decoders, where K represents the number of tasks. Finally, the task prediction vectors $[c_1, c_2, \dots, c_K]$ are generated from the task performers.

III. FEATURE DISTORTION EVALUATION AND IMPORTANCE RANKING

In this section, the FDE network and FIR method are introduced. Firstly, the FDE network is investigated to locate

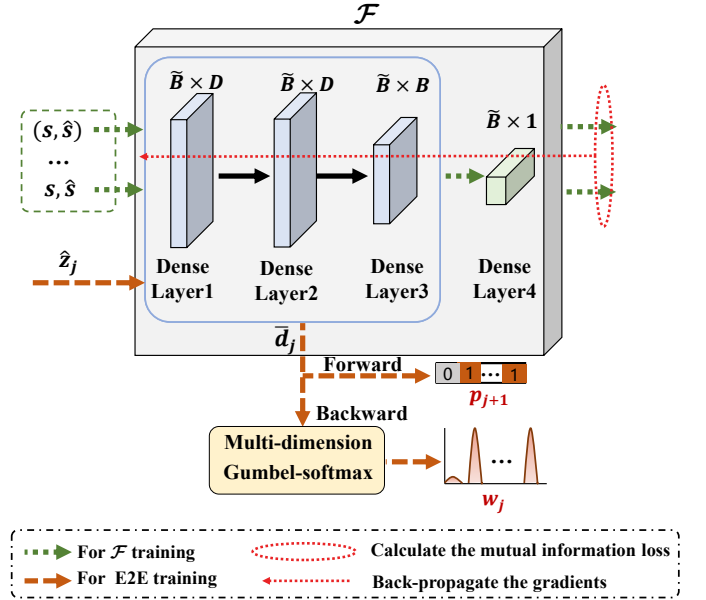


Fig. 3: The structure of the feature distortion evaluation (FDE) network.

the corrupted features that need to be retransmitted in the received feature vector. Then, the FIR method is designed to identify important features in the scalable feature selector for HARQ.

A. Feature distortion evaluation (FDE) network

As shown in Fig. 3, to obtain the distortion extents of the received features, a distortion measure module \mathcal{F} is proposed. Specifically, a neural network (NN) consisting of four dense layers is utilized to evaluate the distortion distribution of the received vector \hat{z}_j after j retransmissions. On this basis, a distortion measure vector is generated by \mathcal{F} during the E2E training, which has the same dimension as \hat{z}_j and indicates the distortion levels of all the features in \hat{z}_j .

To enable \mathcal{F} to distinguish the correlations between input features and the undistorted feature vector \mathbf{s} , thus inferring the distortion extents of these features, \mathcal{F} is trained independently before the entire system training. Since mutual information can be used to measure the semantic similarity between the transmitted and received features, the mutual information of \mathbf{s}

and the JSC-decoded \hat{s} is estimated and serves as the training objective of \mathcal{F} . Consequently, with the parameters optimized by the mutual information, the contributions of different input features to the information recovery can be quantified by \mathcal{F} . The optimization problem is defined as

$$\max_{\xi_{\mathcal{F}}} I(\mathbf{s}; \hat{\mathbf{s}}), \quad (3)$$

where $\xi_{\mathcal{F}}$ is the parameter set of \mathcal{F} . Specifically, the mutual information of \mathbf{s} and $\hat{\mathbf{s}}$ can be calculated by

$$I(\mathbf{s}; \hat{\mathbf{s}}) = \mathbb{E}_{p(\mathbf{s}, \hat{\mathbf{s}})} \left[\log \frac{p(\mathbf{s}, \hat{\mathbf{s}})}{p(\mathbf{s})p(\hat{\mathbf{s}})} \right] = D_{\text{KL}}(p(\mathbf{s}, \hat{\mathbf{s}}) \| p(\mathbf{s})p(\hat{\mathbf{s}})), \quad (4)$$

where $p(\mathbf{s})$ and $p(\hat{\mathbf{s}})$ are the marginal probability of \mathbf{s} and $\hat{\mathbf{s}}$, respectively, and $p(\mathbf{s}, \hat{\mathbf{s}})$ is the joint probability of \mathbf{s} and $\hat{\mathbf{s}}$. Meanwhile, the mutual information is equivalent to the Kullback-Leibler (KL) divergence between the product of the marginal probabilities and the joint probability. Inspired by the general-purpose parametric neural estimation method of mutual information [32], the KL-divergence in (4) obeys the following dual representation,

$$D_{\text{KL}}(p(\mathbf{s}, \hat{\mathbf{s}}) \| p(\mathbf{s})p(\hat{\mathbf{s}})) = \sup_{T: \Omega \rightarrow \mathbb{R}} \mathbb{E}_{p(\mathbf{s}, \hat{\mathbf{s}})}[T] - \log(\mathbb{E}_{p(\mathbf{s})p(\hat{\mathbf{s}})}[e^T]), \quad (5)$$

where the supremum is taken over all functions T . Consequently, the lower bound of $I(\mathbf{s}; \hat{\mathbf{s}})$ can be derived as follows,

$$I(\mathbf{s}; \hat{\mathbf{s}}) = D_{\text{KL}}(p(\mathbf{s}, \hat{\mathbf{s}}) \| p(\mathbf{s})p(\hat{\mathbf{s}})) \geq \mathbb{E}_{p(\mathbf{s}, \hat{\mathbf{s}})}[T] - \log(\mathbb{E}_{p(\mathbf{s})p(\hat{\mathbf{s}})}[e^T]). \quad (6)$$

Due to T can be any class of functions satisfying integrability, the NN in \mathcal{F} is employed as T to obtain a precise bound according to (6). Finally, the estimated mutual information can be denoted as

$$I(\mathbf{s}; \hat{\mathbf{s}} | \mathcal{F}) = \mathbb{E}_{p(\mathbf{s}, \hat{\mathbf{s}})}[\mathcal{F}] - \log(\mathbb{E}_{p(\mathbf{s})p(\hat{\mathbf{s}})}[e^{\mathcal{F}}]), \quad (7)$$

where \mathcal{F} is trained in an unsupervised manner and the optimization goal is updated to maximize $I(\mathbf{s}; \hat{\mathbf{s}} | \mathcal{F})$. Additionally, note that during the training phase of \mathcal{F} , the inputs are generated by sampling from $(\mathbf{s}, \hat{\mathbf{s}})$, \mathbf{s} , and $\hat{\mathbf{s}}$. Moreover, an output vector $\bar{\mathbf{d}}_j$ is obtained by feeding $\hat{\mathbf{z}}_j$ into \mathcal{F} when the entire SemHARQ system is trained, and the distortion measure vector \mathbf{d}_j can be given by $\mathbf{d}_j = 1 - \bar{\mathbf{d}}_j$.

Furthermore, to instruct the transmitter to retransmit the corrupted features, \mathbf{d}_j is quantized into a binary feedback vector \mathbf{p}_{j+1} to trigger the $(j+1)$ -th retransmission. Note that the process is not trivial because the quantization is discrete, which makes the network non-differentiable and hard to optimize with back-propagation. Thus, a straight-through Gumbel-softmax estimator is investigated [33], where \mathbf{d}_j is discretized in the forward pass but a gradient estimator based on Gumbel-softmax distributions is employed to resolve the non-differentiability in the backward pass. Specifically, for the forward propagation, \mathbf{p}_{j+1} is drawn from \mathbf{d}_j using a distortion threshold t , which can be represented as

$$p^{(j+1)i} = \begin{cases} 1 & \text{if } d_{ji} \geq t, \\ 0 & \text{otherwise,} \end{cases} \quad (8)$$

where $p^{(j+1)i}$ and d_{ji} denote the i -th value of \mathbf{p}_{j+1} and \mathbf{d}_j , respectively. On this basis, \mathbf{p}_{j+1} can serve as a feedback vector to guide the next retransmission. Particularly, the number of features requested to be retransmitted is equal to the number of 1 values in \mathbf{p}_{j+1} , which is given by

$$R = \sum_{i=1}^B p^{(j+1)i}, \quad (9)$$

where B is the length of \mathbf{p}_{j+1} .

For the backward propagation, simply back-propagating through the binarization function as if it had been an identity function may cause discrepancies between the forward and backward pass, leading to high variance. Therefore, to improve the efficiency and stability of gradient estimation, Gumbel-softmax distributions are used, where each sample is a differentiable proxy of the corresponding discrete sample. Furthermore, note that straightforwardly applying single-dimension Gumbel-softmax is probable to sample repeatedly since the R selections act independently and are not aware of each other. To solve this issue, a multi-dimension Gumbel-softmax scheme is proposed, where R Gumbel-softmax distributions are designed simultaneously from R categorical distributions generating from \mathbf{d}_j . The R Gumbel-softmax distributions are used to estimate the gradients of R samplings in the forward propagation.

Specifically, a categorical vector $\mathbf{v}_j^r \in \mathbb{R}^B$ is designed for the r -th sampling, where $r = 1, \dots, R$. It is obtained from $\mathbf{d}_j^r \in \mathbb{R}^B$ after a softmax function and can be denoted as

$$\mathbf{v}_j^r = \text{softmax}(\mathbf{d}_j^r), \quad (10)$$

where \mathbf{d}_j^r is obtained after replacing the largest $r-1$ values with 0 in \mathbf{d}_j . On this basis, \mathbf{v}_j^r serves as a probability vector involving the variables in \mathbf{d}_j^r , and can be utilized to form the r -th Gumbel-softmax distribution. Since the samples from Gumbel-softmax distributions will become identical to the samples from the corresponding categorical distributions along with training, the maximum value in each categorical vector will most likely be sampled, matching the forward propagation. Therefore, \mathbf{v}_j^r is used to select the r -th largest value in \mathbf{d}_j , mitigating repetitive samplings. Consequently, the sample vector \mathbf{w}_j^r in r -th sampling is represented as

$$\mathbf{w}_j^r = \text{softmax}\left(\left(\log(\mathbf{v}_j^r) + \mathbf{g}^r\right)/\tau\right), \quad (11)$$

where \mathbf{g}^r is a sampling vector drawn from Gumbel(0,1) distribution. The softmax function in (11) is used as a continuous, differentiable approximation to $\arg \max$, and τ serves as the softmax temperature. As τ approaches 0, the distribution will become more discrete and the sample vectors will converge to one-hot vectors. During training, the temperature parameter is decreased by an exponentially decreasing curve as in [34, 35]. Finally, all the R sample vectors are summed up to be a continuous relaxation of the quantized \mathbf{p}_{j+1} for backward propagation, which is denoted as

$$\mathbf{w}_j = \sum_{r=1}^R \mathbf{w}_j^r. \quad (12)$$

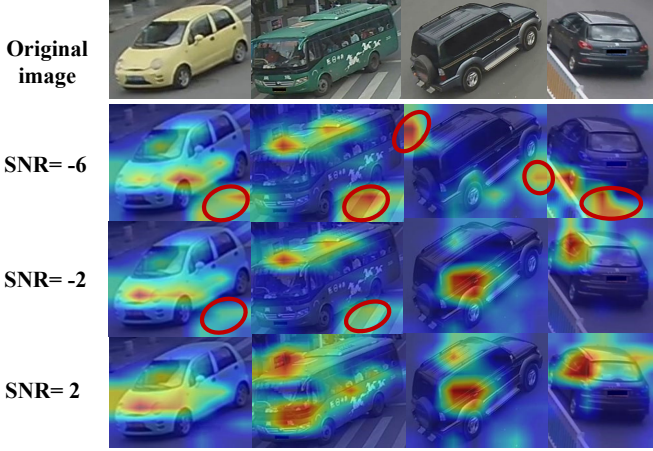


Fig. 4: The gradient-weighted class activation mapping visualization results w.r.t. different channel conditions, where warmer colors indicate contributing semantic features while red circles indicate distracting backgrounds.

B. Feature importance ranking (FIR)

To identify the importance levels of different features in \mathbf{f} w.r.t. specific tasks, we refer to gradient-weighted class activation mapping (Grad-CAM) [36, 37], where visual explanations of the decision-making process of a convolutional neural network (CNN) are proposed. In Grad-CAM, the important regions within an input image are identified by leveraging the gradients flowing into the last convolutional layer of the CNN. The gradients represent the sensitivity of each feature map w.r.t. the target class. The higher the gradient value, the more influential the corresponding feature map is for the prediction.

In this paper, the important features are identified by calculating the gradient of the task predictions relative to the feature vector \mathbf{f} . Intuitively, Fig. 4 demonstrates the visualization results with the proposed SemHARQ architecture of three multi-task, i.e., vehicle re-identification (ReID), vehicle color classification and vehicle type classification, where warmer colors indicate regions with more significance. Apparently, as SNR gets better, SemHARQ focuses more on the vehicles than the backgrounds, leading to better task performance. The specific methodology for calculating the importance levels of semantic features is shown as follows.

Firstly, as shown in Fig. 5, the input images are fed into the proposed SemHARQ to obtain the output logits w.r.t. different tasks, where the entire \mathbf{f} is encoded and transmitted without feature selection. Retransmissions are triggered and guided by the FDE network if the received features fail to pass the detection of the retransmission identification module. Then, the gradients of the target classes w.r.t. the features of \mathbf{f} are calculated by back-propagating the final predictions through the system. Specifically, the probability vector output by the k -th task performer is denoted as $\mathbf{c}_k \in \mathbb{R}^M$, where M indicates the total number of categories of the k -th task. The importance level corresponding to each feature in \mathbf{f} is obtained by calculating the partial derivative of c_{km} relative to \mathbf{f} , where c_{km} is the probability corresponding to the predicted category. The importance measure vector w.r.t. k -th task is then

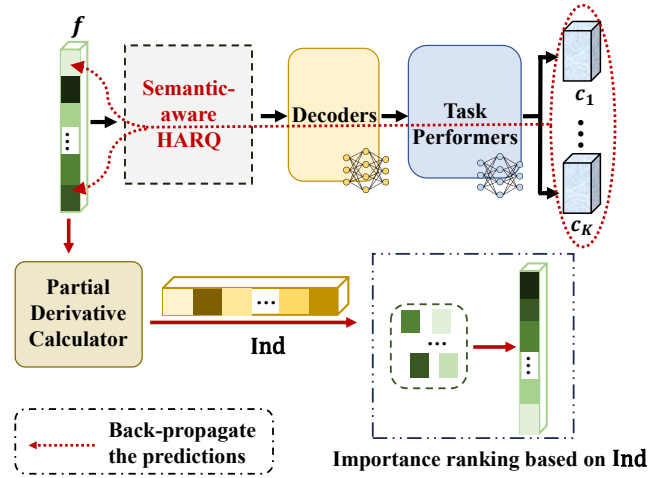


Fig. 5: The framework of feature importance ranking (FIR), where features with deeper colors in \mathbf{f} have higher importance levels.

represented as

$$\tilde{\mathbf{f}}_k = \frac{\partial c_{km}}{\partial \mathbf{f}}, \quad (13)$$

which represents the significance of each feature of \mathbf{f} to the k -th task. Finally, the importance measure vectors of all the K tasks are summed up, and then an integral importance measure vector is obtained,

$$\mathbf{Ind} = \sum_{k=1}^K \lambda_k \tilde{\mathbf{f}}_k, \quad (14)$$

where λ_k denotes the weight of the k -th task, $\tilde{\mathbf{f}}_k$ is the importance measure vector corresponding to the k -th task. In the end, the features in \mathbf{f} are selected based on the importance measure vector \mathbf{Ind} under various channel conditions. The features corresponding to the positions with larger values in \mathbf{Ind} are with higher priority at the first transmission and all the incremental transmissions.

IV. SEMANTIC-AWARE HARQ

In this section, the process of SemHARQ is further analyzed. Meanwhile, the training strategy of SemHARQ is proposed to optimize the training process.

A. SemHARQ

The structure of SemHARQ of j retransmissions is shown in Fig. 6. Firstly, the feature vector to be transmitted at the first transmission is obtained by encoding and scalable feature selection, which is represented by

$$\tilde{\mathbf{z}}_0 = f_{\text{sfs}} \left(C_\alpha \left(S_\beta(\mathbf{x}) \right) \right), \quad (15)$$

where $S_\beta(\cdot)$ and $C_\alpha(\cdot)$ denote the multi-task semantic encoder with the parameter set β and the JSC-Encoder with the parameter set α , respectively, and $f_{\text{sfs}}(\cdot)$ indicates the scalable feature selector, whose structure is shown in Fig. 7. Consequently, $\tilde{\mathbf{z}}_0$ consists of B features chosen from the encoded feature vector according to the importance measure vector \mathbf{Ind} and the given

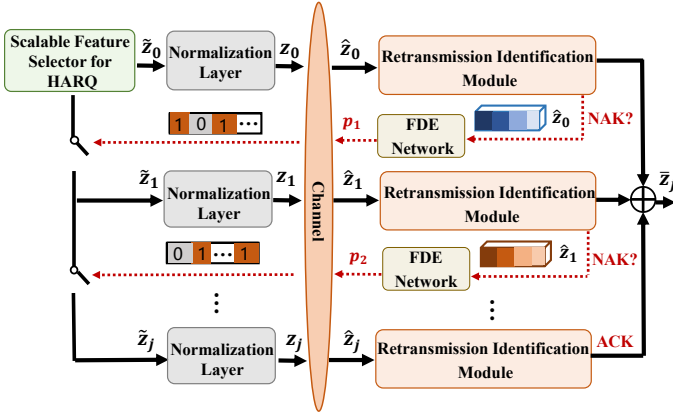


Fig. 6: The structure of SemHARQ.

channel condition. After normalizing and passing through the channel, the received feature vector is represented as \hat{z}_0 at the receiver.

Then, \hat{z}_0 is detected by the retransmission identification module to determine the need for retransmission. Specifically, a retransmission criterion based on the received data uncertainty is applied [12]. Consider the acquisition of a concatenated feature vector \bar{z}_j after j retransmissions, the receiver repeatedly requests the transmitter to retransmit until

$$\overline{\text{SNR}} > \min\left(\theta_0 \mathcal{L}(\mathcal{U}(\bar{z}_j)), \theta_{\text{SNR}}\right), \quad (16)$$

where $\overline{\text{SNR}}$ stands for the receive-SNR after the previous transmissions, $\mathcal{U}(\cdot)$ denotes the received information uncertainty, $\mathcal{L}(\cdot)$ represents a monotonically increasing reshaping function which is set to $\mathcal{L}(x) = 1 + x$, θ_0 indicates a given conversion ratio between the uncertainty and SNR, and θ_{SNR} is a given maximum SNR. Particularly, the receive-SNR is obtained by integrating the information after multiple retransmissions, which is given by

$$\overline{\text{SNR}} = \frac{2P}{\sigma^2} \sum_{i=1}^J |h^{(i)}|^2, \quad (17)$$

where P is the average power of the received semantics, $h^{(i)}$ represents the channel coefficient at i -th retransmission, $\frac{\sigma^2}{2}$ indicates the noise variance, J denotes the total number of transmissions. As for the uncertainty, $\mathcal{U}(\bar{z}_j)$ is measured by the average entropy of the posterior probability distribution corresponding to different tasks. In terms of the k -th task, the uncertainty is given by

$$\mathcal{U}_k(\bar{z}_j) = - \sum_{y_k} p_\gamma(y_k | \bar{z}_j) \log p_\gamma(y_k | \bar{z}_j), \quad (18)$$

where y_k denotes a class label and γ is the set of parameters of the decoders and the task performer to be learned. The uncertainty measures the contribution of the received semantics to the task performance from the perspective of information entropy, and thus serves as a criterion for measuring the adequacy of the amount of received information. Furthermore, since the uncertainty will be constantly bridged by increasing the receive-SNR or equivalently the number of

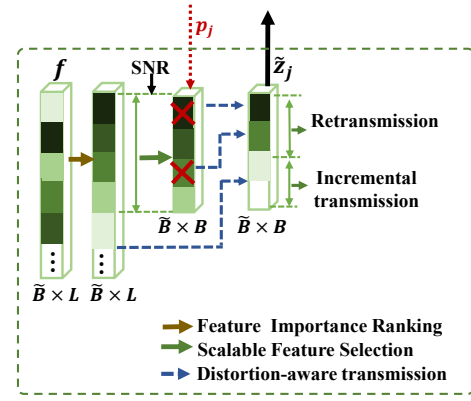


Fig. 7: The structure of the scalable feature selector for HARQ, where the semantic features are transmitted directly after scalable feature selection at the first transmission.

retransmissions, the inequality in (16) is intuitively used to evaluate the adequacy of the number of retransmissions.

After passing through the retransmission identification module, if \hat{z}_0 passes the detection successfully, it is fed into the decoders and the multiple task performers to generate the multi-task predictions. The received feature vector is decoded as

$$\mathbf{c}_k = T_{\phi_k} \left(S_{\beta_k^{-1}}^{-1} \left(C_{\alpha^{-1}}^{-1}(\hat{z}_0) \right) \right), \quad (19)$$

where \mathbf{c}_k denotes the predicted probability vector of the k -th task, $C_{\alpha^{-1}}^{-1}(\cdot)$, $S_{\beta_k^{-1}}^{-1}(\cdot)$ and $T_{\phi_k}(\cdot)$ represent the JSC-Decoder with parameter set α^{-1} , the semantic decoder of the k -th task with parameter set β_k^{-1} and the task performer of the k -th task with parameter set ϕ_k , respectively. Additionally, if \hat{z}_0 fails to pass the detection, the FDE network is utilized to generate the feedback vector p_1 to trigger the first distortion-aware retransmission. The distorted features in \hat{z}_0 are required to be retransmitted according to the distortion evaluation. In particular, the incremental transmission of new features in order of importance levels is combined with the retransmission, further improving the transmission efficiency. Furthermore, after the first retransmission, \hat{z}_1 is obtained at the receiver and concatenated with the cached semantics from the previous transmission. The retransmission process will continue until either the receive-SNR is sufficiently large or the predetermined maximum number of retransmissions is reached.

B. Training strategy

To improve the efficiency of SemHARQ training, a three-stage training strategy is proposed. We focus on three representative tasks in intelligent traffic scenarios for experiments, namely vehicle ReID, vehicle color classification, and vehicle type classification. DenseNet-121 pre-trained on ImageNet is used as the initial model. In the first stage, to improve the performance of feature distortion evaluation, the FDE network is trained with other trainable modules frozen. The training loss can be expressed as,

$$L_{\text{FDE}} = L_{\text{CH}} + L_{\text{MI}}, \quad (20)$$

Algorithm 1 Training process of SemHARQ.

Stage 1: Training of the FDE network.

Input: The semantic encoded s and JSC-decoded \hat{s} , initialized parameters $\xi_{\mathcal{F}}$ of the distortion measure module \mathcal{F} in the FDE network.

Output: $\xi_{\mathcal{F}}$.

- 1: Sample from (s, \hat{s}) , s and \hat{s} , and feed the samples into \mathcal{F} .
- 2: Estimate the mutual information of s and \hat{s} by (7).
- 3: Train $\xi_{\mathcal{F}}$ by loss function $-I(s; \hat{s}|\mathcal{F})$.

Stage 2: Training of the whole HARQ system without scalable feature selection.

Input: Images \mathbf{x} from training dataset, initialized parameters $\alpha, \beta, \alpha^{-1}, \beta_k^{-1}, \phi_k$ with \mathbf{f} fully transmitted; $k = 1, \dots, K$.

Output: $S_{\beta}(\cdot), C_{\alpha}(\cdot), C_{\alpha^{-1}}(\cdot), S_{\beta_k^{-1}}(\cdot), T_{\phi_k}(\cdot)$.

- 1: **Transmitter:** $\mathbf{f} = C_{\alpha}(S_{\beta}(\mathbf{x}))$.
- 2: **while** the retransmission criterion and the maximum number of retransmissions are not met **do**
- 3: Obtain \mathbf{p}_j from the FDE network and
- 4: Send \mathbf{p}_j back to the transmitter.
- 5: Trigger distortion-aware retransmission according to \mathbf{p}_j .
- 6: **end while**
- 7: **Receiver:** $\bar{\mathbf{z}}_j = [\hat{\mathbf{z}}_1, \dots, \hat{\mathbf{z}}_j], \mathbf{c}_k = T_{\phi_k}(S_{\beta_k^{-1}}^{-1}(C_{\alpha^{-1}}^{-1}(\bar{\mathbf{z}}_j)))$.
- 8: Train $\alpha, \beta, \alpha^{-1}, \beta_k^{-1}, \phi_k$ by loss function L_{E2E} ; $k = 1, \dots, K$.
- 9: Calculate the importance measure vector **Ind**.

Stage 3: Retraining of the SemHARQ with scalable feature selection according to **Ind**.

where $L_{\text{CH}}, L_{\text{MI}}$ denote the channel transmission loss and the loss of mutual information, respectively. Specifically, L_{CH} can be measured by the mean square error (MSE),

$$L_{\text{CH}} = \frac{1}{N} \sum_{n=1}^N \|s_n - \hat{s}_n\|_2^2, \quad (21)$$

where s denotes the feature vector extracted by the semantic encoder, and \hat{s} is the feature vector decoded by the JSC-Decoder. The mutual information loss is denoted as

$$L_{\text{MI}} = -I(s; \hat{s}|\mathcal{F}), \quad (22)$$

where $I(s; \hat{s}|\mathcal{F})$ is calculated in (7).

Then, to calculate the feature importance levels, the whole system is trained with the entire \mathbf{f} transmitted without considering the constraint of communication capacity. The overall E2E loss is represented by

$$L_{\text{E2E}} = L_{\text{FDE}} + L_{\text{T}}, \quad (23)$$

where L_{T} is the multi-task loss. Specifically, the losses of the three tasks are weighted, which can be given by

$$L_{\text{T}} = \lambda_r L_r + \lambda_c L_c + \lambda_t L_t, \quad (24)$$

where $L_r, L_c,$ and L_t correspond to the ReID, color classification, and type classification losses, respectively, $\lambda_r, \lambda_c,$ and

λ_t denote the respective task weights. Specifically, L_r consists of the hard-mining triplet loss [38] and the cross-entropy loss, defined as $L_r = \mathcal{L}_{ht}(a, p, n) + \mathcal{L}_{ce}(\mathbf{y}, \hat{\mathbf{y}})$, where a, p and n represent anchor, positive and negative elements, respectively. The hard-mining triplet loss $\mathcal{L}_{ht}(a, p, n)$ is defined as

$$\mathcal{L}_{ht}(a, p, n) = \max \left\{ \left(\max(d_{ap}) - \min(d_{an}) + \alpha \right), 0 \right\}, \quad (25)$$

where d_{ap} and d_{an} denote the distances between the extracted features of the anchor and positive/negative images. $\mathcal{L}_{ce}(\mathbf{y}, \hat{\mathbf{y}})$ indicates the cross-entropy loss, which is defined as

$$\mathcal{L}_{ce}(\mathbf{y}, \hat{\mathbf{y}}) = \sum_{k=1}^K y_k \log(\hat{y}_k) + (1 - y_k) \log(1 - \hat{y}_k), \quad (26)$$

where \mathbf{y} denotes the label of the task and $\hat{\mathbf{y}}$ is the predicted one. For the other two classification tasks, the cross-entropy loss is also employed.

Finally, the SemHARQ considering scalable feature selection is trained based on **Ind** with limited bandwidth and time slot, where all the trainable parameters are optimized. The most important B features are transmitted, where B is determined by channel conditions. The pseudocode of the whole training process is shown in Algorithm 1.

V. NUMERICAL RESULTS

In this section, simulations are performed to evaluate the proposed system. The details of the simulation settings and the structure of the network are introduced. Then, the proposed SemHARQ is compared with other baselines, and the results are analyzed.

A. Dataset and performance metrics

The adopted dataset is VeRi-776 [39], which contains over 50,000 images of 776 vehicles captured by 20 cameras covering an area of 1.0 square kilometers, making the dataset flexible to be used for vehicle ReID and other related tasks. The images are captured in unconstrained surveillance scenarios and are labeled with different attributes such as vehicle type, color, and brand. Thus, the evaluation results are all presented based on the VeRi-776 dataset.

Two of the most popular metrics, rank-1 accuracy and mean average precision (mAP), are used to evaluate the performance of vehicle ReID. Specifically, rank-1 accuracy measures the percentage of query images that are correctly matched at the top-ranked position based on the similarity or distance metrics. The mAP represents the mean of the AP, indicating the proportion of the correctly retrieved gallery images in the gallery image set. It evaluates the identification performance in a more global view. Additionally, the other two classification tasks are evaluated by the average accuracy.

B. Simulation settings and numerical analysis

The detailed network settings of the proposed SemHARQ are shown in Table I. The system is evaluated under several SNR levels and the average power budget P is set to 1. During training, the input images are first resized to 256×256 .

TABLE I: The network settings of SemHARQ.

Transmission System	Modules	Layer	Output dimensions	Activation function
Transmitter	Input	\mathbf{x}	256×256	/
	Multi-task semantic encoder	DenseNet-121	1024	ReLU
	JSC-Encoder	FC with BN	1024	Leaky ReLu
		FC	1024	Linear
	Scalable feature selector for HARQ	/	B	/
Output (j -th retransmission)		$\tilde{\mathbf{z}}_j$	B	/
Channel	Rician fading	/	/	/
Receiver	Input	$\hat{\mathbf{z}}_j$	B	/
	Retransmission identification	NACK or concatenation	/ or $B \times (j + 1)$	/
	JSC-Decoder	FC with BN	1024	Leaky ReLu
		FC	1024	ReLU
	Semantic decoder 1 for vehicle ReID	FC	1024	Leaky ReLu
	Semantic decoder 2 for vehicle color classi.	FC	512	Leaky ReLu
	Semantic decoder 3 for vehicle type classi.	FC	512	Leaky ReLu
	Task performer 1 for vehicle ReID	FC	575	/
	Task performer 2 for vehicle color classi.	FC	10	/
	Task performer 3 for vehicle type classi.	FC	9	/
Output		$\mathbf{c}_1, \mathbf{c}_2, \mathbf{c}_3$	575, 10, 9	/
FDE network (j -th retransmission)	\mathcal{F}	Dense Layer 1	256	ReLU
		Dense Layer 2	256	ReLU
		Dense Layer 3	B	Sigmoid
		Dense Layer 4	1	/
	Mutual information estimation	/	1	/
	Multi-dimension Gumbel-softmax	\mathbf{p}_j	B	/

¹ FC: fully connected layer; BN: batch normalization; ReLu: rectified linear unit.

² The retransmission identification module sends NACK to the FDE network if the detection is not successful, otherwise, concatenates the received vector with the buffered feature vectors.

DenseNet-121 is utilized as our backbone deep neural network (DNN), which is optimized by Adam [40]. $\lambda_r, \lambda_c, \lambda_t$ are set to 1, 0.125, 0.125, respectively. The training batch and testing batch are set to 16 and 100, respectively. Besides, the learning rate is initialized as $1e-4$, and learning rate decay is applied. By adjusting the distortion threshold t in III-A, the number of features to be retransmitted is approximately the same as those for incremental transmission on average. In addition, the given conversion ratio θ_0 in IV-A is set to 1 dB, and the given maximum SNR θ_{SNR} can be determined by $\theta_{\text{SNR}} = \theta_0 [1 + \log M]$, where $\log M$ is the maximum entropy, M denotes the total number of categories.

The proposed E2E system is compared with the state-of-the-art HARQ benchmarks. The details are as follows:

- Traditional II-HARQ method: JPEG, LDPC with $\frac{3}{4}$ rate and 16 QAM are used for source coding, channel coding and modulation, respectively. Then, the CRC is employed at the receiver and the incremental redundancy information is requested to transmit when CRC fails until the success or the maximum number of transmissions is reached. After the image reconstruction, the three intelligent tasks are performed using DenseNet121.
- Semantic-aware HARQ baselines: 1) IK-S-HARQ [9]: An incremental knowledge-based semantic-aware HARQ method is compared. Specifically, the B features to be transmitted are incrementally selected from \mathbf{f} at each

transmission in order of the importance level. 2) RT-S-HARQ [12]: A retransmission-only semantic-aware HARQ method is compared, where the most important B features are selected and retransmitted at each transmission.

Note that the IK-S-HARQ and RT-S-HARQ are both DL-based and JSCC is applied to achieve the best results.

Fig. 8 presents the vehicle ReID performance w.r.t. different methods. It is obvious that the semantic-aware HARQ methods outperform the traditional method in both rank-1 accuracy and mAP, which verifies the superiority of SemCom in transmitting the meaning of information efficiently. Furthermore, the proposed SemHARQ achieves the best performance among three semantic-aware HARQ methods, followed by IK-S-HARQ and RT-S-HARQ. The rank-1 accuracy gaps between SemHARQ and IK-S-HARQ and RT-S-HARQ at -2 dB are 18.50% and 30.97%, respectively, while in terms of the mAP, the gaps are 21.78% and 43.61%, respectively. The gain is attributed to the precise evaluation of the feature distortion in SemHARQ, where only distorted features are allowed to be retransmitted, improving the efficiency of channel resource utilization significantly. Note that the percentage of mAP is generally lower than the rank-1 accuracy. For example, the rank-1 accuracy of SemHARQ is 68.22%, yet the corresponding mAP is only 42.94% at -2 dB. The reason is that mAP combines accuracy and recall for different categories of the recognition task,

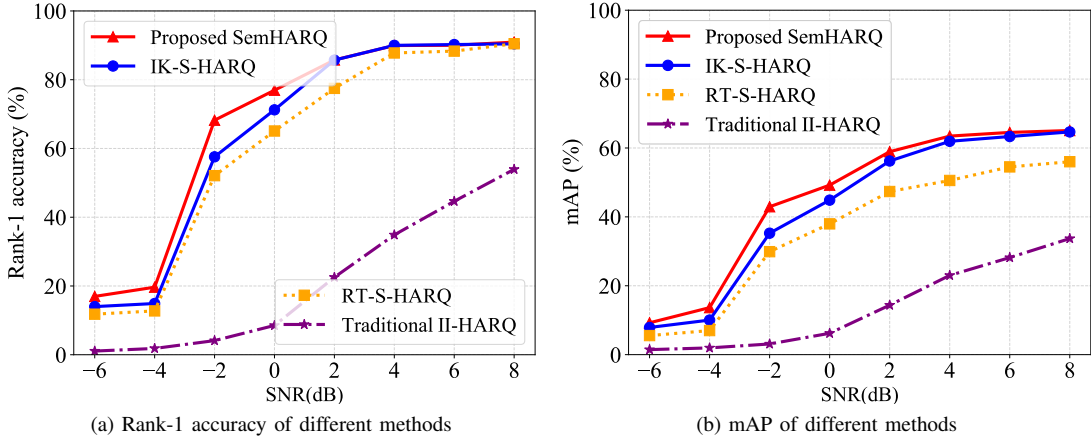


Fig. 8: Rank-1 accuracy and mAP of vehicle ReID w.r.t. different methods.

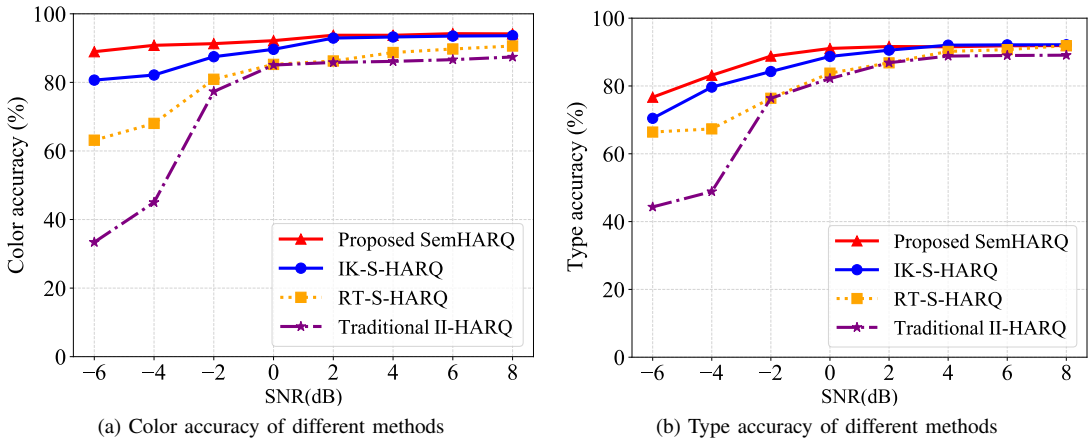


Fig. 9: Accuracy of vehicle color classification and type classification w.r.t. different methods.

which is usually more rigorous than rank-1 accuracy.

At the same time, the accuracy of the other two classification tasks is illustrated in Fig. 9. The performance of SemHARQ is superior to other methods, especially at low SNR regime. Specifically, at -6 dB, in terms of color classification, SemHARQ improves the performance by 10.28%, 40.88% and 166.48%, compared with the IK-S-HARQ, the RT-S-HARQ and the traditional HARQ, respectively. For type classification, the performance is improved by 8.83%, 15.46%, and 73.01%, respectively. Note that the performance gain progressively reduces as SNR increases, which results from the correct reception of most of the information under good channel conditions. On this basis, the retransmissions become less meaningful.

To further verify the effectiveness of the FDE network in SemHARQ, we conduct an ablation study for comparison. The distorted features are directly identified from the received feature vector \hat{z}_j using multi-dimension Gumbel-softmax in the comparison method. Accordingly, \mathcal{F} and mutual information estimation discussed in III-A are not involved, and FDE network training is not taken into account. As shown in Fig. 10, the multi-task accuracy w.r.t. different channel condi-

tions is demonstrated. It shows that our proposed SemHARQ achieves better task performance, especially with poor SNRs. Specifically, at -6 dB, the multi-task performance has been improved by 67.52%, 2.69%, and 13.01% by using the FDE network, respectively. The reason is that the FDE network enhances the distortion evaluation ability of the system by measuring the contribution of the received semantics to the mutual information at each transmission. The obtained distortion levels quantify the degree of feature distortion, providing precise guidance on retransmission. Therefore, the efficiency of retransmission is improved dramatically.

The impact of FIR is also presented in Table II. The task performance is compared with the sequentially selected transmission (SST) method which transmits the first B features without considering the importance levels at each transmission. Both FIR and SST perform scalable transmission w.r.t. various SNR levels. It is obvious that the FIR method surpasses the SST method significantly for all three tasks. Particularly, at -2 dB, the recognition accuracy increases by 155.91%, 11.02%, and 8.11% in the three tasks, respectively. Note that vehicle ReID is more challenging due to the high intra-class variability coupled with small inter-class variability. However,

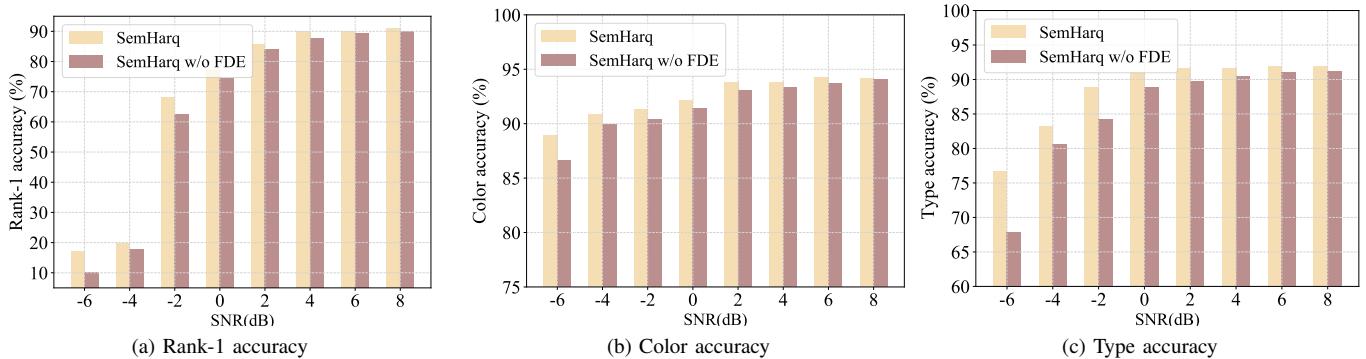


Fig. 10: Multi-task accuracy comparison between SemHARQ and SemHARQ without FDE, w.r.t. SNR.

TABLE II: Performance comparison of the proposed FIR method and the SST method.

SNR (dB)	Proposed FIR (%)			SST (%)		
	Rank-1 acc.	Color acc.	Type acc.	Rank-1 acc.	Color acc.	Type acc.
-6	16.97	88.95	76.68	1.61	42.54	47.51
-4	19.65	90.81	83.15	5.96	70.76	70.54
-2	71.22	91.30	88.81	27.83	82.24	82.15
0	79.94	92.17	91.07	68.00	90.72	87.67
2	85.74	93.75	91.64	83.91	92.67	90.97
4	89.94	93.75	91.75	88.97	92.80	91.45
6	90.01	94.21	91.85	89.52	93.47	91.29
8	90.94	94.55	91.92	90.01	93.54	91.54

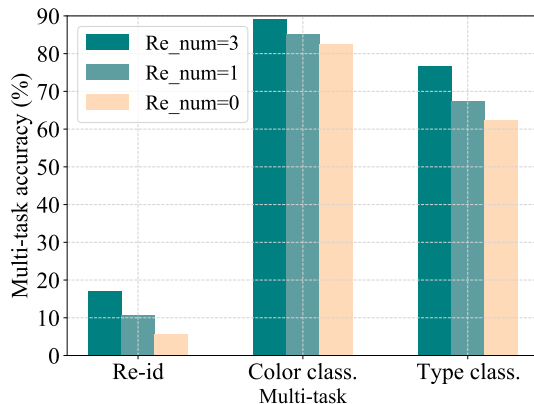


Fig. 11: The impact of retransmissions on the accuracy of multi-task.

greater advancements are made on the vehicle ReID than the remaining two tasks, demonstrating the superiority of the proposed system. One of the reasons is that the proposed FIR can build the relationship between the importance distribution of the semantic information and the multi-task predictions, thus effectively finding the optimal feature selection policy for partial semantics transmissions.

Besides, to validate the effectiveness of the proposed SemHARQ more comprehensively, the gain of the system is investigated by increasing the number of retransmissions progressively. Fig. 11 presents the impact of retransmissions on the task performance in the case of SNR = -6 dB. Note that as the number of retransmissions increases, the system performance improves obviously. Particularly, the performance of vehicle ReID after three retransmissions is almost triple than that of the no-retransmission method, which further proves the validity of SemHARQ.

Moreover, to confirm the effectiveness of the retransmission identification module, the average numbers of retransmissions are summarized in Fig. 12 w.r.t. multiple SNR levels, where the maximum number is set large enough. As shown in Fig. 12, the retransmissions are more frequent under harsh channel conditions to meet the criteria in (16). The average number of retransmissions at -6 dB is almost 18 times higher than at 8 dB when θ_0 , the given conversion ratio between the uncertainty and SNR, is set to 1 dB. Meanwhile, the need for retransmissions reduces when θ_0 becomes lower accordingly,

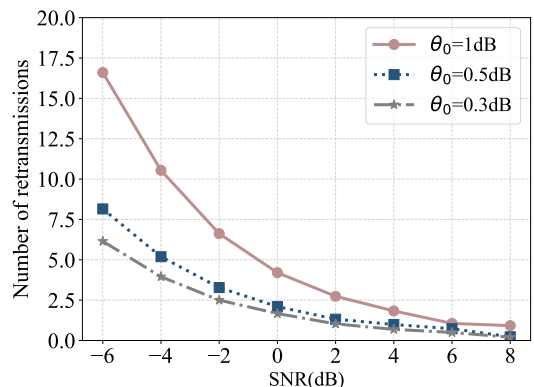


Fig. 12: Average number of retransmissions after using the retransmission identification module.

which represents that the receiver's demand for necessary information reception has been decreased.

VI. CONCLUSIONS

In this paper, a novel semantic-aware HARQ framework SemHARQ is proposed for multi-task semantic communications. Specifically, the task-related semantics are extracted by a multi-task semantic encoder and scalably transmitted in descending order of importance levels. On this basis, to enable the SemHARQ and improve the semantic error correction of the system, the distortion level of each received feature is

evaluated by a feature distortion evaluation (FDE) network. The corrupted features are identified by the distortion measure vector and retransmitted by the transmitter. Meanwhile, the incremental transmission is triggered to fully utilize the channel resources. Compared with the existing semantic-aware and traditional HARQ methods, the proposed SemHARQ has improved the multi-task performance by 16.27%-166.48% at low SNR regime.

REFERENCES

- [1] C. W. Morris, "Foundations of the theory of signs," in *International encyclopedia of unified science*. Chicago University Press, 1938, pp. 1–59.
- [2] C. E. Shannon, "A mathematical theory of communication," *The Bell system technical journal*, vol. 27, no. 3, pp. 379–423, 1948.
- [3] W. Weaver, "Recent contributions to the mathematical theory of communication," *ETC: a review of general semantics*, pp. 261–281, 1953.
- [4] H. Xie, Z. Qin, G. Y. Li, and B.-H. Juang, "Deep learning enabled semantic communication systems," *IEEE Transactions on Signal Processing*, vol. 69, pp. 2663–2675, 2021.
- [5] Y. Zheng, F. Wang, W. Xu, M. Pan, and P. Zhang, "Semantic communications with explicit semantic base for image transmission," *ArXiv preprint*, vol. abs/2308.06599, 2023.
- [6] E. Bourtsoulatze, D. B. Kurka, and D. Gündüz, "Deep joint source-channel coding for wireless image transmission," *IEEE Transactions on Cognitive Communications and Networking*, vol. 5, no. 3, pp. 567–579, 2019.
- [7] W. Xu, Y. Zhang, F. Wang, Z. Qin, C. Liu, and P. Zhang, "Semantic communication for the internet of vehicles: A multiuser cooperative approach," *IEEE Vehicular Technology Magazine*, vol. 18, no. 1, pp. 100–109, 2023.
- [8] J. Shao, Y. Mao, and J. Zhang, "Learning task-oriented communication for edge inference: An information bottleneck approach," *IEEE Journal on Selected Areas in Communications*, vol. 40, no. 1, pp. 197–211, 2021.
- [9] Q. Zhou, R. Li, Z. Zhao, Y. Xiao, and H. Zhang, "Adaptive bit rate control in semantic communication with incremental knowledge-based harq," *IEEE Open Journal of the Communications Society*, vol. 3, pp. 1076–1089, 2022.
- [10] J. Laneman, G. Wornell, and D. Tse, "An efficient protocol for realizing cooperative diversity in wireless networks," in *Proceedings. 2001 IEEE International Symposium on Information Theory (IEEE Cat. No.01CH37252)*, 2001.
- [11] J. Laneman, D. Tse, and G. Wornell, "Cooperative diversity in wireless networks: Efficient protocols and outage behavior," *IEEE Transactions on Information Theory*, vol. 50, no. 12, pp. 3062–3080, 2004.
- [12] D. Liu, G. Zhu, Q. Zeng, J. Zhang, and K. Huang, "Wireless data acquisition for edge learning: Data-importance aware retransmission," *IEEE transactions on wireless communications*, vol. 20, no. 1, pp. 406–420, 2020.
- [13] D. B. Kurka and D. Gündüz, "Deepjssc-f: Deep joint source-channel coding of images with feedback," *IEEE Journal on Selected Areas in Information Theory*, vol. 1, no. 1, pp. 178–193, 2020.
- [14] M. Nakahara, M. Nishimura, Y. Ushiku, T. Nishio, K. Maruta, Y. Nakayama, and D. Hisano, "Edge computing-assisted dnn image recognition system with progressive image retransmission," *IEEE Access*, vol. 10, pp. 91 253–91 262, 2022.
- [15] X. Bao, M. Jiang, and H. Zhang, "Adjscc-l: Snr-adaptive jscc networks for multi-layer wireless image transmission," in *2021 7th International Conference on Computer and Communications (ICCC)*, 2021, pp. 1812–1816.
- [16] D. B. Kurka and D. Gündüz, "Successive refinement of images with deep joint source-channel coding," in *2019 IEEE 20th International Workshop on Signal Processing Advances in Wireless Communications (SPAWC)*, 2019, pp. 1–5.
- [17] P. Jiang, C.-K. Wen, S. Jin, and G. Y. Li, "Deep source-channel coding for sentence semantic transmission with harq," *IEEE transactions on communications*, vol. 70, no. 8, pp. 5225–5240, 2022.
- [18] Jiang, Peiwen and Wen, Chao-Kai and Jin, Shi and Li, Geoffrey Ye, "Wireless semantic communications for video conferencing," *IEEE Journal on Selected Areas in Communications*, vol. 41, no. 1, pp. 230–244, 2022.
- [19] J. Hu, F. Wang, W. Xu, H. Gao, and P. Zhang, "Scalable multi-task semantic communication system with feature importance ranking," in *ICASSP 2023 - 2023 IEEE International Conference on Acoustics, Speech and Signal Processing (ICASSP)*, 2023, pp. 1–5.
- [20] Y. Wang, M. Chen, T. Luo, W. Saad, D. Niyato, H. V. Poor, and S. Cui, "Performance optimization for semantic communications: An attention-based reinforcement learning approach," *IEEE Journal on Selected Areas in Communications*, vol. 40, no. 9, pp. 2598–2613, 2022.
- [21] Y. Wang, M. Chen, W. Saad, T. Luo, S. Cui, and H. V. Poor, "Performance optimization for semantic communications: An attention-based learning approach," in *2021 IEEE Global Communications Conference (GLOBECOM)*, 2021, pp. 1–6.
- [22] Z. Xiao, S. Yao, J. Dai, S. Wang, K. Niu, and P. Zhang, "Wireless deep speech semantic transmission," in *ICASSP 2023 - 2023 IEEE International Conference on Acoustics, Speech and Signal Processing (ICASSP)*, 2023, pp. 1–5.
- [23] J. Sun, C. Jia, and Z. Shi, "Vehicle attribute recognition algorithm based on multi-task learning," in *2019 IEEE International Conference on Smart Internet of Things (SmartIoT)*, 2019, pp. 135–141.
- [24] Z. Tang, M. Naphade, S. Birchfield, J. Tremblay, W. Hodge, R. Kumar, S. Wang, and X. Yang, "PAMTRI: pose-aware multi-task learning for vehicle re-identification using highly randomized synthetic data," in *2019 IEEE/CVF International Conference on Computer Vision, ICCV 2019, Seoul, Korea (South), October 27 - November 2, 2019*, 2019, pp. 211–220.
- [25] X. Cheng, W. Xu, Z. Yao, Z. Zhu, Y. Li, H. Li,

- and Y. Zou, “FC-MTLF: A Fine- and Coarse-grained Multi-Task Learning Framework for Cross-Lingual Spoken Language Understanding,” in *Proc. INTERSPEECH 2023*, 2023, pp. 690–694.
- [26] Y. Zhang and Q. Yang, “A survey on multi-task learning,” *IEEE Transactions on Knowledge and Data Engineering*, vol. 34, no. 12, pp. 5586–5609, 2022.
- [27] X. Cheng, Q. Dong, F. Yue, T. Ko, M. Wang, and Y. Zou, “M 3 st: Mix at three levels for speech translation,” in *ICASSP 2023-2023 IEEE International Conference on Acoustics, Speech and Signal Processing (ICASSP)*. IEEE, 2023, pp. 1–5.
- [28] X. Cheng, B. Cao, Q. Ye, Z. Zhu, H. Li, and Y. Zou, “MI-lmcl: Mutual learning and large-margin contrastive learning for improving asr robustness in spoken language understanding,” in *Findings of the Association for Computational Linguistics: ACL 2023*, 2023, pp. 6492–6505.
- [29] H. Wei, W. Xu, F. Wang, X. Du, T. Zhang, and P. Zhang, “Semaudio: Semantic-aware streaming communications for real-time audio transmission,” in *GLOBECOM 2022-2022 IEEE Global Communications Conference*, 2022, pp. 3965–3970.
- [30] Y. Zhang, W. Xu, H. Gao, and F. Wang, “Multi-user semantic communications for cooperative object identification,” in *2022 IEEE International Conference on Communications Workshops (ICC Workshops)*, 2022, pp. 157–162.
- [31] Q. Sun, C. Guo, Y. Yang, J. Chen, R. Tang, and C. Liu, “Deep joint source-channel coding for wireless image transmission with semantic importance,” in *2022 IEEE 96th Vehicular Technology Conference (VTC2022-Fall)*, 2022, pp. 1–7.
- [32] M. I. Belghazi, A. Baratin, S. Rajeswar, S. Ozair, Y. Bengio, R. D. Hjelm, and A. C. Courville, “Mutual information neural estimation,” in *Proceedings of the 35th International Conference on Machine Learning, ICML 2018*, pp. 530–539.
- [33] E. Jang, S. Gu, and B. Poole, “Categorical reparameterization with gumbel-softmax,” in *5th International Conference on Learning Representations, ICLR 2017*.
- [34] T. Strypsteen and A. Bertrand, “End-to-end learnable eeg channel selection for deep neural networks with gumbel-softmax,” *Journal of Neural Engineering*, vol. 18, no. 4, p. 0460a9, 2021.
- [35] A. Abid, M. F. Balin, and J. Zou, “Concrete autoencoders for differentiable feature selection and reconstruction,” *ArXiv preprint*, vol. abs/1901.09346, 2019.
- [36] R. R. Selvaraju, M. Cogswell, A. Das, R. Vedantam, D. Parikh, and D. Batra, “Grad-cam: Visual explanations from deep networks via gradient-based localization,” in *IEEE International Conference on Computer Vision, ICCV 2017*, pp. 618–626.
- [37] S. Xu, D. Chang, J. Xie, and Z. Ma, “Grad-cam guided channel-spatial attention module for fine-grained visual classification,” in *2021 IEEE 31st international workshop on machine learning for signal Processing (MLSP)*. IEEE, 2021, pp. 1–6.
- [38] A. Hermans, L. Beyrer, and B. Leibe, “In defense of the triplet loss for person re-identification,” *ArXiv preprint*, vol. abs/1703.07737, 2017.
- [39] X. Liu, W. Liu, T. Mei, and H. Ma, “A deep learning-based approach to progressive vehicle re-identification for urban surveillance,” in *Computer Vision—ECCV 2016: 14th European Conference, Amsterdam, The Netherlands, October 11-14, 2016, Proceedings, Part II 14*. Springer, 2016, pp. 869–884.
- [40] D. P. Kingma and J. Ba, “Adam: A method for stochastic optimization,” in *3rd International Conference on Learning Representations, ICLR 2015*.